UNIQUELY ORIENTING DRY MICRO ASSEMBLY BY TWO-STAGE SHAPE RECOGNITION

Jiandong Fang, Karl F. Böhringer
Department of Electrical Engineering, University of Washington, Seattle, WA 98195 USA

ABSTRACT

We demonstrate a completely dry, uniquely orienting and parallel micro assembly method on the basis of two-stage shape recognition between complementary features on parts and receptor sites. A dry environment benefits assembly of chips with either exposed movable microstructures or materials sensitive to liquid environments; uniquely orienting self-alignment based on complementary features works for any part shape; parallel assembly greatly increases throughput for mass production. In our experiments, 1mm square dummy silicon parts were assembled with a defect rate of ~2% in 10 minutes on each of two assembly templates having respectively 397 and 720 receptor sites. This assembly technique enables either wafer level packaging of micro device chips or easy part feeding and palletizing for robotic assembly systems without constraints of part shapes or materials.

Keywords: Micro assembly, unique self-alignment, two-stage shape recognition.

INTRODUCTION

Micro assembly is a key process for both packaging of micro device chips and integration of complex hybrid micro systems. Current micro assembly techniques can be categorized into four major types: micromanipulator based assembly [1], wafer-to-wafer device transfer [2], fluidic shape-directed self-assembly [3], and capillary-driven self-assembly [4, 5]. Each of these assembly techniques has its limitations: micromanipulator based assembly processes are serial and slow, and micro parts tend to stick to micromanipulators because adhesive forces dominate gravitational forces; wafer-to-wafer device transfer can only be applied to microstructures monolithically fabricated on the same substrate; most types of micro device chips are in rectangular shapes due to mechanical dicing along straight lines, but neither fluidic shape-directed self-assembly nor capillary-driven self-assembly can align them to a unique in-plane orientation, which is required, for example, for a microchip with multiple interconnect pads or polarity so that correct electrical connections can be established via flip-chip bonding to a chip carrier substrate.

In the field of robotic assembly, many methods have been developed to orient bulk parts for part feeders. Vibratory bowl methods [6] pick parts with desired orientations via track filters. Programmable squeezing fields [7] uniquely orient some types of flat polygonal parts. Neither of these two methods can uniquely orient parts with rotational symmetries such as rectangular and circular parts. Usually visual feedback systems are used for flexible part feeders ("flexible" means that multiple types of parts can be handled by a single feeder) to present parts with correct orientations [8]. But all these part feeding methods are serial processes and not suitable for very large numbers of parts, e.g. mass packaging of radio frequency identification (RFID) chips.

Virtually all current assembly techniques having parallel assembly capabilities are performed in aqueous environments, e.g. fluidic shape-directed self-assembly and capillary-driven self-assembly [9]. In an aqueous environment, liquid flow transports parts to receptor sites and carries away unassembled parts from the assembly template. But for microchips with exposed movable microstructures, a dry assembly process is a better choice because these microstructures are easily stuck by surface tension of liquid residue from a wet assembly process. A dry assembly process is also required for microchips with materials and coatings sensitive to aqueous environments.

We focus our research on completely dry, uniquely orienting and parallel assembly of micro parts on an alignment template (ALT). We base the dry assembly process on a mechanism of two-stage shape recognition to obtain unique in-plane orientation for each part: the first shape recognition causes a part to be anchored to a receptor site, and the second one fixes the anchored part to a specific in-plane orientation. The two-stage shape recognition is performed between protruding features on the part and complementary recessed patterns on the receptor site. We have demonstrated the assembly of 388 and 710 1mm square dummy silicon parts within 10 minutes respectively on a ∅100mm ALT with a polar array of 397 receptor sites and a ∅100mm ALT with an orthogonal array of 720 receptor sites. Each assembly process had a ~98% yield. For simplicity, we describe the complete assembly process only for the 397-receptor-site ALT in the following sections.

FABRICATION

The complete assembly process is schematically shown in Fig. 1. Dummy silicon parts with dimension 1mm×1mm×0.5mm were used for demonstration. The protruding features on the part are a circular peg (CP) offset from the center of mass and a cross peg (XP): the dimension of the longer XP beam is 1mm×50μm×35μm, and the diameter and height of the CP are 200μm and 65μm, respectively. The recessed features for the receptor site have complementary shapes with greater dimensions for easier shape-matching: a cross trench (XT) is 40μm greater in width than the XP, and the diameter of the circular trench (CT) is 300μm greater

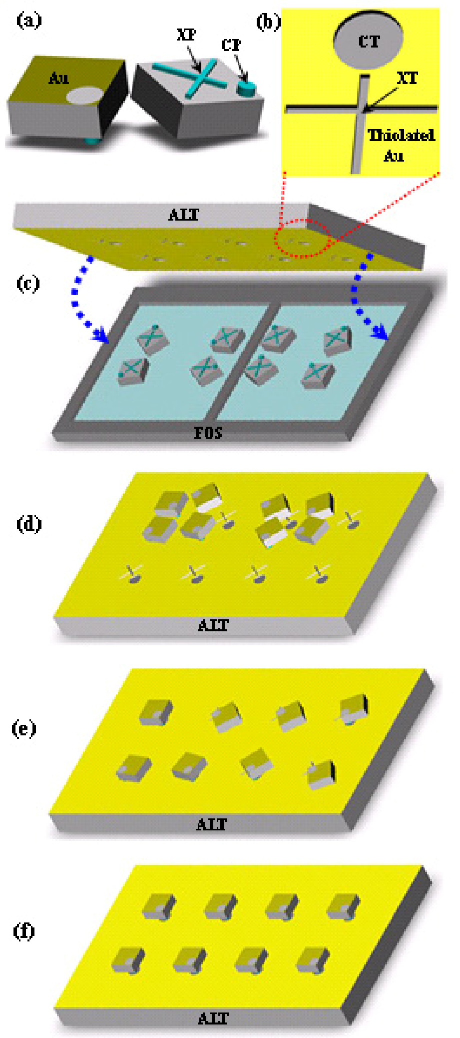

Fig. 1: Schematic overview of the dry process to parallel assemble square micro parts. **(a)** Top and bottom views of a silicon part: the bottom face has a CP and an XP, and the CP has twice the height of the XP; the top face is coated with gold, and the opening in the gold layer marks the position of the CP. **(b)** Trenches of a receptor site on the ALT. **(c)** Bulk parts face-oriented on an orbitally shaken FOS and then sandwiched by adding an ALT. **(d)** Parts palletized to the ALT with their peg sides facing downwards. **(e)** Parts one-to-one anchored to receptor sites by orbital shaking: the CPs fall into the CT (1st shape recognition). **(f)** Parts rotated by orbital shaking introduced torques until their XPs fall into the XTs (2nd shape recognition).

than that of the CP, and both the XT and CT are 70µm in depth. We fabricated the CPs and XPs with different heights on a ∅100mm silicon substrate by using two subsequent deep reactive ion etching (DRIE) processes: a layer of 3900Å thermal oxide was grown on the silicon substrate and patterned by wet etching in buffered oxide etchant (BOE) to be left only on the XP areas, then photoresist AZ4620 was spincoated and patterned to be a DRIE mask protecting only the CP areas, and the patterned oxide acted as a DRIE mask with a very slow etching rate (approximately 1% of silicon etching rate) during the 1st DRIE and was completely removed by BOE before the 2nd DRIE, therefore the heights of the XPs and CPs were respectively determined by the 1st DRIE and both DRIEs. After the pegs were fabricated on the silicon substrate, we deposited a layer of TiW/Au (50/800Å) on the backside of the silicon substrate and patterned it via double-sided lithography to form marks indicating the positions of the CPs or the part polarity (Fig. 1a). Finally the ∅100mm silicon substrate was diced into 1mm square silicon parts by a mechanical dicing saw. An array of 70µm deep receptor site trenches on a ∅100mm silicon substrate was fabricated by a single DRIE process.

THE SELF-ASSEMBLY PROCESS

The first step for the assembly process is to uniquely face-orient bulk parts on a face-orienting substrate (FOS). The FOS has an array of large square wells, which confine parts locally. We fabricated the FOS out of an oxidized ∅100mm silicon substrate with TAMH etching: oxide was first patterned to produce the silicon etching mask, and 4 hours etching at 90°C resulted in 240µm deep wells. Initially bulk silicon parts were stored in a glass container with random face orientations. We harnessed orbital shaking to face-orient bulk silicon parts: 600 parts (about 50% redundant parts for the 397-receptor-site ALT, aiming for a high assembly yield) were poured onto a FOS attached to the platform of an orbital shaker (51300 Series, Cole-Parmer Instr. Co., IL, USA) with an approximately uniform distribution. Then the shaker ran at 200RPM for about 1 minute and the centrifugal force flipped over all but 4 tilted parts onto their flat faces, while all the other parts stayed resting on their flat faces. All the remaining 4 tilted parts were kept immobile by surrounding parts (Fig. 2a). In order to face-orient bulk parts and keep them locally confined, the orbital shaker needs to be run within a narrow speed range of about 50RPM: a speed higher than 230RPM can cause parts moving across the FOS, and a speed lower than 180RPM cannot flip the tilted parts. The upper and lower speed limits are respectively determined by the FOS well depth and the part tilt angle or the ratio between the peg height and the part side length.

The second step is to palletize the uniquely face-oriented parts to an ALT (Fig. 2b). We placed the ALT with its receptor sites facing the FOS to sandwich the parts, and turned them over. Thereby, the patterned ridges on the FOS kept the parts in place. Then we removed the FOS, and 99% of the parts were transferred to the ALT except very few parts sticking to the FOS due to adhesive forces.

The final step is to assemble the palletized parts to the receptor sites with unique in-plane orientations. We utilized a mechanism based on two-stage shape recognition to assemble these parts. To reduce sliding friction of the silicon ALT, we deposited a layer of

TiW/Au (50/800Å) and soaked the ALT in 1mmol alkanethiol $CH_3(CH_2)_{11}SH$ (in ethanol) solution for the Au surface to adsorb a self-assembled monolayer (SAM). The thiolated gold surface has a friction coefficient of about 0.04 [10], one order of magnitude less than that of a silicon surface. To reduce friction effects even further, we attached the ALT to an ultrasonic stage mounted on an orbital shaker. To move the parts around without flipping over, the orbital shaker was run in a speed range whose limits were given as follows: the lower speed limit introduced a centrifugal force just enough to overcome the stationary friction; the upper speed limit caused the tilted parts to flip over. We ran the orbital shaker at 110RPM. The moving parts were first anchored to the receptor sites when their CPs fell into the CTs, and came to rest horizontally on their XPs. Because the CPs were offset from the centers of mass, the centrifugal force from orbital shaking exerted torques on the anchored parts to drive them to rotate about their CPs until their XPs fell into the XTs; at this point the parts were fixed to the uniquely defined in-plane orientations. After 10 minutes agitation, 388 receptor sites were correctly registered with parts, which indicated a yield of 97.7% (Fig. 2c-d). We removed the unassembled parts from the ALT by tilting the ultrasonic stage so that gravity drove them to slide away.

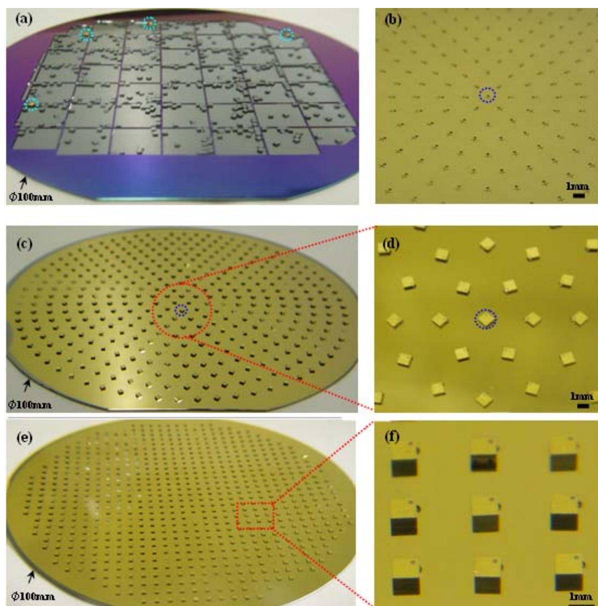

Fig. 2: Optical photographs of templates and assembly results. **(a)** After 1 minute of orbital shaking, only 4 silicon parts stay tilted by their pegs on the $\emptyset$100mm FOS. **(b)** A partial view of an ALT with a polar array of receptor sites. **(c)** 388 silicon parts assembled on the $\emptyset$100mm ALT with a polar array of 397 receptor sites. **(d)** Zoom-in view of the center of the ALT. **(e)** 710 silicon parts assembled on the $\emptyset$100mm ALT with an orthogonal array of 720 receptor sites. **(f)** Zoom-in view of a 3 × 3 section of the array of receptor sites.

We also assembled the same silicon parts on a $\emptyset$100mm ALT with 720 receptor sites according to the above process steps. 50% redundant parts were used. 710 parts were correctly assembled within 10 minutes, i.e., the assembly yield reached 98.6% (Fig. 2e-f).

During the assembly, we noticed two types of defects: (1) occasionally unassembled parts adhered to the assembled parts; (2) parts resting on their flat faces were immobile during the agitation, which blocked other moving parts. The part sticking was mainly caused by contamination from the previous process steps. Because the face-orienting process did not have perfect 100% yield, some parts rested on their flat faces after palletizing. We manually removed these parts to avoid the 2nd type of defects. In addition, we kept the vibration intensity of the ultrasonic stage low enough to prevent parts from flipping over.

CONCLUSION AND DISCUSSION

We have demonstrated assembly of 1mm square silicon parts, and our assembly strategy can also be applied to flat parts of any shape with a larger or smaller scale if the following design rules are observed. (1) The CP is offset from the center of mass and higher than the XP. (2) The CT has a greater diameter than the CP for fast anchoring of parts, but the CT diameter has an upper

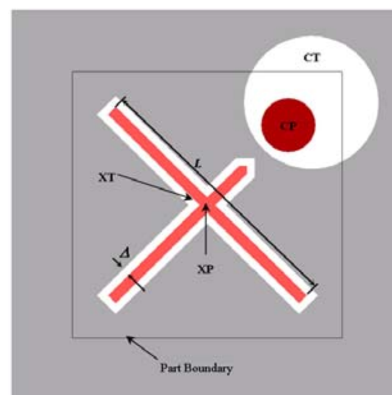

Fig. 3: Schematic top view of the exact alignment between a part and a receptor site. The clearance between the XP and XT determines maximum alignment error.

limit, which prevents two CPs of two neighboring parts or one XP from entering one CT, i.e., one CT is assigned exclusively to one CP to guarantee one-to-one registration and correct alignment. (3) The XT has a greater width than the XP beam to anchor the XP quickly, but a smaller width than the diameter of the CP to exclude the CP. (4) The space between receptor sites is large enough for two neighboring parts to rotate without blocking each other and unassembled parts to slide through it. From the exact alignment layout (Fig. 3), we can determine the maximum misalignments: the maximum translational misalignment is equal to the clearance Δ between the XT and XP, and the maximum rotational misalignment is $tan^{-1}(2\Delta/L)$, where L is the length of the longer XP beam. Clearance Δ is chosen for the XP to enter the XT easily and is independent of the part size, while L can be as large as possible to obtain a minimum rotational misalignment. For the previous two

assemblies of 1mm square diced silicon parts, clearance Δ is 20μm, and $tan^{-1}(2\Delta/L)$ is about 2°.

Our assembly process is also applicable to parts made of non-silicon materials, when combined with additive fabrication techniques for the two high-aspect-ratio pegs with different heights. We demonstrated this by fabricating the CPs and XPs out of negative photoresist SU8-2025 (MicroChem Corp., MA, USA) with the following major fabrication process steps: (1) 1st layer of SU8 was spincoated and UV light exposed with a mask having transparent areas for XPs; (2) 2nd layer of SU8 was spincoated and UV light exposed with a mask having transparent areas for CPs; (3) SU8 was developed, and finally only the CPs and XPs exposed by UV light were left on the substrate.

Adhesive and friction forces, which are the major causes for potential failures of our assembly technique, become more significant compared with gravitational forces for smaller parts. Our assembly method has been demonstrated with 1mm square parts, and we believe that it can assemble larger device chips with dimension up to centimeters which are less affected by adhesive forces. In micro domains, both the adhesive and frictional forces are approximately proportional to contact area. The adhesive forces come mainly from electrostatic interactions, van der Waals attractive forces and surface tension from adsorbed moisture on the part and the substrate [11]. The gold face of the ALT can eliminate the electrostatic charges at the bottom faces of parts, but not the charges at the sidewalls of parts, which can cause parts sticking to each other. A photoionizer can effectively neutralize electrostatic charges on any exposed surface by introducing ions into the surrounding atmosphere. Adsorbed moisture can be reduced by heating the ALT or performing the assembly in a vacuum environment. With good control of environment humidity, electrostatic charges and sliding friction, we believe that our assembly process can handle parts of much smaller size.

Our assembly mechanism itself applies no upper limit on the ALT size. All the agitations required in the assembly process are orbital shaking, which introduces centrifugal forces evenly distributed all across the shaker platform. The orbital shaker platform supported by three rotating arms can be easily expanded. High-aspect-ratio trench features on the ALT can be fabricated with many available techniques such as DRIE (only for silicon ALT), molding, and others. These trench fabrication techniques limit the ALT size.

Previously we reported a wafer level packaging method using a semi dry and uniquely orienting self-assembly process [12]. The completely dry self-assembly process combined with flip-chip bonding techniques can also be utilized to package micro device chips at the wafer level with the same packaging strategy: (1) interconnect pads are placed on the flat face of the part; (2) an array of parts are correctly registered to receptor sites on an ALT with their interconnect pads facing upwards; (3) the aligned parts are bonded to a chip carrier substrate by wafer level flip-chip bonding. In addition to these applications in wafer level packaging of integrated circuits and micro electromechanical systems, we expect that our assembly technique without constraints on part shapes or materials can also be exploited as part feeding and palletizing for robotic assembly systems.

ACKNOWLEDGMENTS

This work is funded by NIH Center of Excellence in Genomic Science and Technology grant 1-P50-HG002360-01. Karl Böhringer was supported in part by a fellowship from the Japan Society for the Promotion of Science.

REFRENCES

[1] M. B. Cohn, K. F. Böhringer, J. M. Noworolski, A. Singh, C. G. Keller, K. Y. Goldberg, R. T. Howe, "Microassembly technologies for MEMS," *Proc. SPIE Micromachining and Microfabrication, Santa Clara, CA, USA, Sept. 20-22*, pp. 2, 1998.

[2] M. B. Cohn, Y. C. Liang, R. T. Howe, A. P. Pisano, "Wafer-to-wafer transfer of microstructures for vacuum packaging," *Solid-state Sensor and Actuator Workshop, Hilton Head Island, SC, USA, June 2-6*, 1996.

[3] H. J. Yeh, J. S. Smith, "Fluidic Self-Assembly for the Integration of GaAs Light-Emitting Diodes on Si Substrates," *IEEE Photonics Technol. Lett.*, vol. 6, pp. 706, 1994.

[4] H. O. Jacobs, A. R. Tao, A. Schwartz, D. H. Gracias, G. M. Whitesides, "Fabrication of Cylindrical Display by Patterned Assembly," *Science*, vol. 296, pp. 323, 2002.

[5] J. Fang, K. Wang, K. F. Böhringer, "Self-assembly of micro pumps with high uniformity in performance," *Solid State Sensor, Actuator, and Microsystems Workshop, Hilton Head Island, SC, June 6-10*, 2004.

[6] G. Boothroyd, C. Poli, L. Murch, *Automatic Assembly, Marcel Dekker, Inc.*, 1982.

[7] K. F. Böhringer, B. R. Donald, N. C. MacDonald, "Programmable Vector Fields for Distributed Manipulation, with Applications to MEMS Actuator Arrays and Vibratory Parts Feeders," *International Journal of Robotics Research*, vol. 18, pp. 168, 1999.

[8] S. Sorensen, R. Stringham, "Feature Vision guided flexible feeding made easy," *Industrial Robot*, vol. 26, pp. 99, 1999.

[9] U. Srinivasan, D. Liepmann, R. T. Howe, "Microstructure to Substrate Self-Assembly Using Capillary Forces," *J. Microelectromechanical Systems*, vol. 10, pp. 17, 2001.

[10] S. Jiang, "Molecular simulation studies of self-assembled monolayers of alkanethiols on Au(111)," *Molecular Physics*, vol. 100, pp. 2261, 2002.

[11] R. S. Fearing, "Survey of Sticking Effects for micro parts," *IEEE Int. Conf. Robotics and Intelligent Systems IROS '95, Pittsburgh, PA August 7-9*, 1995.

[12] J. Fang, K. F. Böhringer, "High yield batch packaging of micro devices with uniquely orienting self-assembly," *IEEE Conference on Micro Electro Mechanical Systems (MEMS), Miami Beach, FL, Jan. 30 - Feb. 3*, 2005.